Fourth International Accelerator School for Linear Colliders

Beijing, September 2009

Course A4: Damping Ring Design and Physics Issues

Lecture 4

Damping Wigglers and Nonlinear Dynamics

Andy Wolski

University of Liverpool and the Cockcroft Institute

Damping wigglers and nonlinear dynamics

In this lecture, we shall discuss:

- The use of wigglers to enhance radiation damping.
- The impact of wigglers on equilibrium beam sizes.
- The nonlinear effects of wiggler fields.
- Dynamic aperture and the requirements for damping rings.
- Analysis methods for nonlinear dynamics.

Summary from Lecture 2: radiation damping

Including the effects of radiation damping and quantum excitation, the emittances vary as:

$$\varepsilon(t) = \varepsilon(0)\exp\left(-\frac{2t}{\tau}\right) + \varepsilon(\infty)\left[1-\exp\left(-\frac{2t}{\tau}\right)\right]$$

The damping times are given by:

$$j_x\tau_x = j_y\tau_y = j_z\tau_z = 2\frac{E_0}{U_0}T_0$$

The damping partition numbers are given by:

$$j_x = 1-\frac{I_4}{I_2} \qquad j_y = 1 \qquad j_z = 2+\frac{I_4}{I_2}$$

The energy loss per turn is given by:

$$U_0 = \frac{C_\gamma}{2\pi}E_0^4 I_2 \qquad C_\gamma = 8.846\times10^{-5}\ \text{m/GeV}^3$$

Summary from Lecture 2: synchrotron radiation integrals

The synchrotron radiation integrals are:

$$I_1 = \oint \frac{\eta_x}{\rho}\,ds$$

$$I_2 = \oint \frac{1}{\rho^2}\,ds$$

$$I_3 = \oint \frac{1}{|\rho|^3}\,ds$$

$$I_4 = \oint \frac{\eta_x}{\rho}\left(\frac{1}{\rho^2}+2k_1\right)ds \qquad k_1 = \frac{e}{P_0}\frac{\partial B_y}{\partial x}$$

$$I_5 = \oint \frac{\mathcal{H}_x}{|\rho|^3}\,ds \qquad \mathcal{H}_x = \gamma_x\eta_x^2 + 2\alpha_x\eta_x\eta_{px} + \beta_x\eta_{px}^2$$

Damping times in the ILC damping rings

Let us consider the damping time that we need in the ILC. The shortest damping time is set by the vertical emittance of the positron beam.

	Injected emittance	Extracted emittance
Horizontal e^+	1 μm	0.8 nm
Vertical e^+	1 μm	0.002 nm
Longitudinal e^+	> 30 μm	10 μm

We must reduce the injected emittance to the extracted emittance in the store time of 200 ms (set by the repetition rate of the main linac).

Using:

$$\varepsilon(t) = \varepsilon(0)\exp\left(-2\frac{t}{\tau}\right)$$

we find that we need a vertical damping time of 30 ms. In practice, the damping time must be less than this, to allow for a non-zero equilibrium.

Damping times in the ILC damping rings

The ILC damping rings are 6.7 km in circumference and have a beam energy of 5 GeV.

The energy loss per turn is:

$$U_0 = \frac{C_\gamma}{2\pi} E_0^4 I_2$$

If the only dipole fields are those that determine the ring geometry, and have field strength B, then we can write:

$$I_2 = \oint \frac{1}{\rho^2}\, ds = \frac{B}{B\rho}\oint \frac{ds}{\rho} = 2\pi\frac{eB}{P_0}$$

Hence:

$$U_0 = C_\gamma E_0^3 ecB$$

For a dipole field of 0.15 T, we find U_0 = 500 keV.

Damping times in the ILC damping rings

The beam energy is 5 GeV; the energy loss per turn from the dipoles is 500 keV. This means that the vertical damping time is:

$$\tau_y = 2\frac{E_0}{U_0}T_0 = 450\ \text{ms}$$

We need a damping time of less than 30 ms; the radiation from the dipoles provides a damping time of 450 ms!

To reduce the damping time, we need to increase the energy loss per turn. Increasing the dipole field can help, but has adverse impact on other aspects of the dynamics (the momentum compaction factor is reduced, which lowers some of the instability thresholds).

The other option is to use a *damping wiggler*, which consists of a sequence of dipoles bending in opposite directions…

Wigglers consist of a sequence of dipole magnets

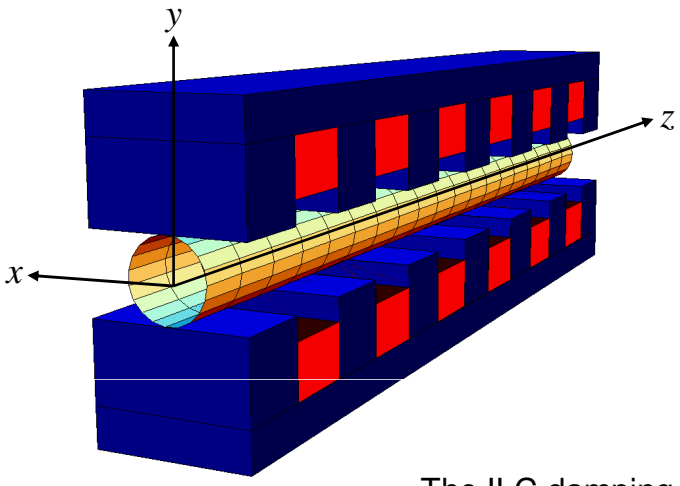

$$B_y = B_w \sin(k_z z)$$

Peak field = B_w

Period = $\lambda_w = \frac{2\pi}{k_z}$

The ILC damping rings specify wigglers with peak field ≈ 1.6 T and period 40 cm.

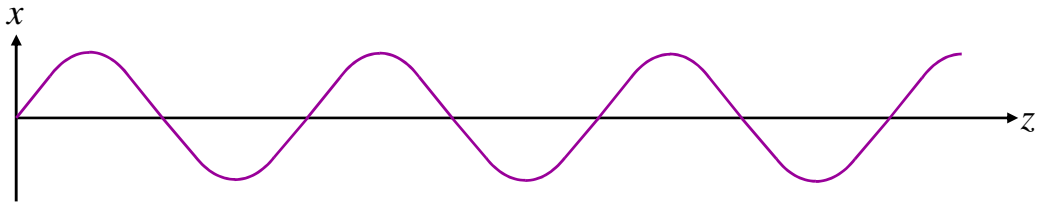

An electromagnetic wiggler (from the KEK-ATF)

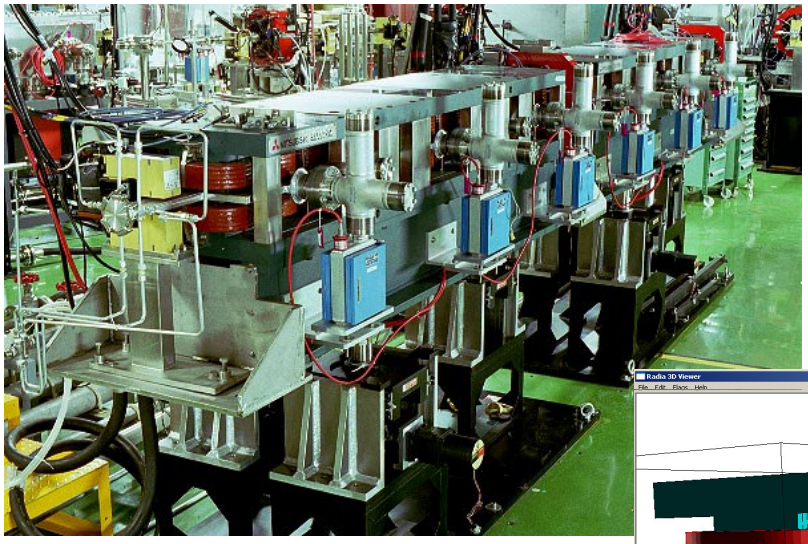

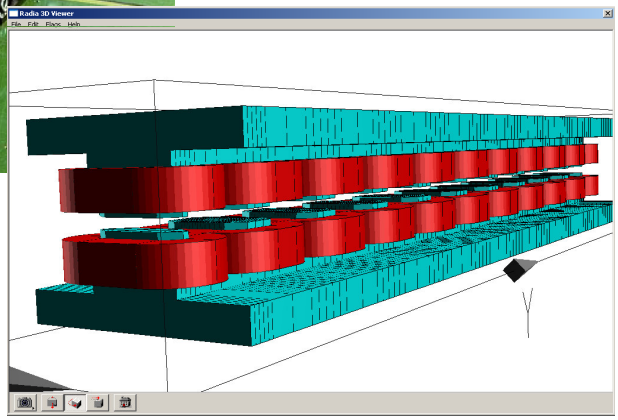

Wigglers increase the energy loss from synchrotron radiation

By contributing additional dipole field, wigglers increase the energy loss of particles from synchrotron radiation.

Since the integrated field over the length of a wiggler is (ideally) zero, wigglers can be inserted into straight sections in the ring, without changing the overall geometry.

The total energy loss per turn is still given in terms of the second synchrotron radiation integral:

$$U_0 = \frac{C_\gamma}{2\pi} E_0^4 I_2 \qquad I_2 = \oint \frac{1}{\rho^2}\, ds$$

But we now have a contribution from the wigglers:

$$I_{2w} = \int_0^{L_w} \frac{1}{\rho^2}\, ds = \frac{1}{(B\rho)^2} \int_0^{L_w} B^2\, ds = \frac{1}{(B\rho)^2} \frac{B_w^2 L_w}{2}$$

Note that I_{2w} depends only on the peak field and the total length of wiggler (and the beam energy), and is independent of the wiggler period.

What length of wiggler do we need in the ILC damping rings?

With a beam energy of 5 GeV and a circumference of 6.7 km, to achieve a damping time of 25 ms, we need an energy loss per turn of:

$$U_0 = 2E_0 \frac{T_0}{\tau_y} = 8.9\,\text{MeV}$$

The dipoles provide an energy loss per turn of 500 keV (assuming 0.15 T dipole field), so the wigglers must provide an energy loss per turn of 8.4 MeV, or 94% of U_0:

$$\frac{C_\gamma}{2\pi} E_0^4 I_{2w} = 8.4\,\text{MeV} \qquad \Rightarrow \qquad I_{2w} = 0.95\,\text{m}^{-1}$$

Hence:

$$\frac{1}{(B\rho)^2} \frac{B_w^2 L_w}{2} = 0.95\,\text{m}^{-1}$$

Assuming a wiggler peak field of 1.6 T, the total length of wiggler required is:

$$L_w \approx 210\,\text{m}$$

Impact of wigglers on the ILC damping rings

We expect the wigglers in the ILC damping rings to provide nearly 95% of the energy loss per turn. The wigglers clearly make a dominant contribution to I_2; it is likely that they also dominate over the dipoles for some of the other synchrotron radiation integrals.

We have to consider the impact of the wigglers on the equilibrium beam sizes…

Wiggler contribution to the momentum compaction factor

The momentum compaction factor α_p (which affects – for example – the synchrotron tune) can be written in terms of the first synchrotron radiation integral:

$$I_1 = \oint \frac{\eta_x}{\rho} ds \qquad \alpha_p = \frac{1}{C_0} I_1 \qquad \omega_s^2 = -\frac{eV_{RF}}{E_0} \frac{\omega_{RF}}{T_0} \alpha_p \cos\varphi_s$$

For a FODO lattice, we can make a rough approximation for the momentum compaction factor:

$$\alpha_p \approx \frac{1}{\nu_x^2}$$

where ν_x is the horizontal tune, which we can estimate from:

$$\nu_x \approx \frac{1}{2\pi} \frac{C_0}{\beta_x}$$

If we assume 6.7 km circumference for the damping rings, and $\beta_x \approx 25$ m, we expect the momentum compaction factor in the damping rings in the absence of any wiggler to be:

$$\alpha_p \approx 5 \times 10^{-4}$$

Wiggler contribution to the momentum compaction factor

To find the contribution of the wiggler to the momentum compaction factor, we need to know the dispersion in the wiggler.

In a dipole of bending radius ρ and quadrupole gradient k_1, the dispersion obeys the equation:

$$\frac{d^2\eta_x}{ds^2} + K\eta_x = \frac{1}{\rho} \qquad K = \frac{1}{\rho^2} + k_1$$

Assuming that $k_1 = 0$ in the wiggler, we can write the equation for η_x as:

$$\frac{d^2\eta_x}{ds^2} + \frac{B_w^2}{(B\rho)^2} \eta_x \sin^2 k_w s = \frac{B_w}{B\rho} \sin k_w s$$

We try a solution:

$$\eta_x \approx \eta_0 \sin k_w s$$

For $k_w \rho_w >> 1$, we can neglect the second term on the left, and we find:

$$\eta_x \approx -\frac{\sin k_w s}{\rho_w k_w^2}$$

Note that for the ILC damping wiggler, $k_w \rho_w \approx 160$.

Wiggler contribution to the momentum compaction factor

Note that we have assumed the only contribution to the dispersion in the wiggler comes from the bending in the wiggler itself. If there is some steering in the wiggler (e.g. from badly aligned quadrupoles) then there will be additional contributions to the dispersion: here, we neglect such contributions.

The dispersion generated by the wiggler itself is very small:

$$|\eta_0| \approx \frac{1}{\rho_w k_w^2}$$

where $\rho_w = (B\rho)/B_w$. For the ILC damping wiggler, we find:

$$|\eta_0| \approx 0.39 \text{ mm}$$

which is to be compared with dispersion of order 10 cm or more in the main arc dipoles. Thus, we expect the wiggler to make only a small contribution to the first synchrotron radiation integral, compared to the main dipoles.

Wiggler contribution to the momentum compaction factor

Now that we know how the dispersion varies along the wiggler, we can write for the wiggler contribution to I_1:

$$I_{1w} = \int_0^{L_w} \frac{\eta_x}{\rho}\, ds \approx -\int_0^{L_w} \frac{\sin^2 k_w s}{\rho_w^2 k_w^2}\, ds = -\frac{L_w}{2\rho_w^2 k_w^2}$$

Note that I_{1w} is negative: this means that particles with a higher energy have a shorter path length in the wiggler. This is (as expected) the opposite situation from the behaviour of the path length in a circular beam line.

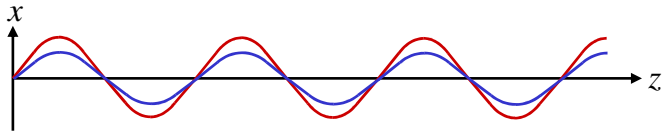

For the ILC damping wiggler parameters, we have $k_w \rho_w \approx 160$, so for a total wiggler length $L_w \approx 210$ m, we find:

$$I_{1w} \approx -\frac{L_w}{2\rho_w^2 k_w^2} \approx -0.004 \text{ m}$$

This is very small compared to the $I_1 \approx 3.4$ m from the dipoles: so the damping wiggler makes negligible contribution to the momentum compaction factor.

Wiggler contribution to the natural energy spread

The natural energy spread is given in terms of the second and third synchrotron radiation integrals:

$$\sigma_\delta^2 = C_q \gamma^2 \frac{I_3}{j_z I_2} \qquad I_3 = \oint \frac{1}{|\rho|^3} ds \qquad C_q = 3.832 \times 10^{-13} \text{ m}$$

Since I_3 does not depend on the dispersion, the wiggler potentially makes a significant contribution to the energy spread. Writing for the bending radius in the wiggler:

$$\frac{1}{\rho} = \frac{B}{B\rho} = \frac{B_w}{B\rho} \sin k_w s = \frac{1}{\rho_w} \sin k_w s$$

we find:

$$I_{3w} = \frac{1}{\rho_w^3} \int_0^{L_w} \left| \sin^3 k_w s \right| ds = \frac{4 L_w}{3\pi \rho_w^3}$$

For the ILC damping wiggler parameters ($L_w \approx 210$ m, $\rho_w \approx 10.4$ m), we find:

$$I_{3w} \approx 0.079 \text{ m}^{-2}$$

This is large compared to the main dipole contribution $\approx 5.1 \times 10^{-4}$ m^{-2}.

Wiggler contribution to the natural energy spread

In the ILC damping rings, the damping wiggler contribution to I_2 and I_3 dominates over the contribution from the dipoles. Therefore, the natural energy spread of the beam in the damping rings is essentially determined by the wiggler:

$$\sigma_\delta^2 \approx \frac{4}{3\pi} C_q \frac{\gamma^2}{\rho_w} = \frac{4}{3\pi} \frac{e}{mc} C_q \gamma B_w$$

The natural energy spread increases in proportion to the square root of the beam energy and the wiggler field.

In the ILC, the energy spread in the beam extracted from the damping rings is an important parameter for the bunch compressors: the larger the energy spread, the more difficult the design and operation of the bunch compressors.

With a beam energy of 5 GeV and a wiggler field of 1.6 T, the natural energy spread in the damping rings is approximately 0.13%. This is acceptable for the bunch compressors: an upper limit would be around 0.15%.

Wiggler contribution to the natural emittance

The natural emittance depends on the second and fifth synchrotron radiation integrals:

$$\varepsilon_0 = C_q \gamma^2 \frac{I_5}{j_x I_2} \qquad C_q = 3.832\times10^{-13}\ \text{m}$$

$$I_2 = \oint \frac{1}{\rho^2}\, ds \qquad I_5 = \oint \frac{\mathcal{H}_x}{|\rho|^3}\, ds \qquad \mathcal{H}_x = \gamma_x \eta_x^2 + 2\alpha_x \eta_x \eta_{px} + \beta_x \eta_{px}^2$$

The contribution of the wiggler to I_5 depends on the beta function in the wiggler. Let us assume that the beta function is constant (or changing slowly), so $\alpha_x \approx 0$. Then, since:

$$\eta_{px} \approx \frac{d\eta_x}{ds} = k_w \eta_0 \cos k_w s$$

and we can assume that:

$$k_w >> \frac{1}{\beta_x}$$

we can approximate:

$$\mathcal{H}_x \approx \frac{\beta_x}{\rho_w^2 k_w^2} \cos^2 k_w s$$

Wiggler contribution to the natural emittance

The wiggler contribution to I_5 can be written:

$$I_{5w} \approx \frac{\langle \beta_x \rangle}{\rho_w^2 k_w^2} \int_0^{L_w} \frac{\cos^2 k_w s}{|\rho|^3}\, ds = \frac{\langle \beta_x \rangle}{\rho_w^5 k_w^2} \int_0^{L_w} \left|\sin^3 k_w s\right| \cos^2 k_w s\, ds$$

Using:

$$\left\langle \left|\sin^3 k_w s\right| \cos^2 k_w s \right\rangle = \frac{4}{15\pi}$$

we have:

$$I_{5w} \approx \frac{4}{15\pi} \frac{\langle \beta_x \rangle L_w}{\rho_w^5 k_w^2}$$

Wiggler contribution to the natural emittance

Assuming $\langle\beta_x\rangle \approx 10$ m, and using the usual wiggler parameters $L_w \approx 210$ m, $\rho_w \approx 10.4$ m and $k_w \approx 15.7$ m^{-1}, we find:

$$I_{5w} \approx 5.9\times10^{-6}\ \text{m}^{-1}$$

How does this compare with the contribution from the main dipoles? In a TME lattice tuned for minimum emittance, I_5 is given by:

$$I_5 = \frac{\pi}{6\sqrt{15}}\frac{\theta^3}{\rho}$$

where θ is the bending angle of one dipole, and ρ is the bending radius. Assuming 120 dipoles with field 0.15 T and a beam energy of 5 GeV, ($\rho_w \approx 111$ m) gives for the main dipole contribution:

$$I_{5D} \approx 1.7\times10^{-7}\ \text{m}^{-1}$$

For the contribution to I_5, the wiggler again dominates over the dipoles. However, a practical TME lattice is often "detuned" from the strict conditions for minimum emittance, and the dipole contribution can be significant. In other lattice styles (e.g. FODO lattice), the dipoles can dominate.

Wiggler contribution to the natural emittance

Combining expressions for I_{2w} and I_{5w}, and assuming that the wiggler dominates the contributions to I_2 and I_5, we can write for the natural emittance:

$$\varepsilon_0 \approx \frac{8}{15\pi} C_q \gamma^2 \frac{\langle\beta_x\rangle}{\rho_w^3 k_w^2}$$

Using the usual parameters for the ILC damping rings, we find:

$$\varepsilon_0 \approx 0.22\ \text{nm}$$

If the dipole contribution is comparable to the wiggler contribution, the natural emittance will be larger than this by roughly a factor of two.

Wiggler contribution to the natural emittance

If the wiggler provides a dominant contribution to the synchrotron radiation integrals I_2 and I_5, then the natural emittance of the lattice will be:

$$\varepsilon_0 \approx \frac{8}{15\pi} C_q \gamma^2 \frac{\langle \beta_x \rangle}{\rho_w^3 k_w^2}$$

It may be necessary, during the design of the lattice, to reduce the natural emittance to allow for contribution from the dipoles, or to allow for collective effects that increase the emittance. A reduction in the wiggler contribution to the emittance can be achieved by:

- reducing the horizontal beta function;
- reducing the wiggler period (i.e. increasing k_w): this reduces the dispersion in the wiggler, hence reducing the quantum excitation;
- reducing the wiggler field (i.e. increasing ρ_w): the length of wiggler then needs to be increased to compensate the loss of damping.

Dynamical effects of wigglers

Wigglers are used in damping rings to enhance the production of synchrotron radiation, and hence reduce the damping times. As we have seen, wigglers also affect the equilibrium energy spread and the natural emittance.

Wigglers have two other effects:

1. Wiggler fields provide linear focusing forces, which must be included in the linear lattice design.

2. Wigglers have non-linear field components that affect particle motion at large amplitude, and can limit the dynamic aperture of the lattice.

Both of these effects are important, so we shall take a closer look at each of them.

3D field in an "ideal" wiggler

Earlier, we wrote the field in the wiggler considering only the vertical component. To satisfy Maxwell's equations, the field must have other components. If the poles of the wiggler are infinitely wide, then we can assume that the horizontal field component vanishes. The simplest field that has a sinusoidal dependence on the longitudinal coordinate is then:

$$B_x = 0$$
$$B_y = B_w \sin k_z z \cosh k_z y$$
$$B_z = B_w \cos k_z z \sinh k_z y$$

Note that on the mid-plane of the wiggler ($y = 0$), this reduces to the field we assumed when calculating the synchrotron radiation integrals.

Since B_z is non-zero for $y \neq 0$, and the particle generally has non-zero horizontal velocity because of the horizontal bending in the vertical field, a particle travelling through the wiggler off the mid-plane will experience a vertical deflecting force.

Let's calculate this force, and its effect on the trajectory of a particle…

Vertical focusing in a wiggler

To simplify the analysis, we will assume that the trajectory of the particle is essentially that determined by the vertical field component in the wiggler. We will treat the effect of other forces (e.g. vertical deflections) as perturbations to that trajectory.

The horizontal equation of motion of a particle on the mid-plane is:

$$\frac{d^2x}{ds^2} = \frac{B_y}{B\rho} = \frac{B_w}{B\rho} \sin k_z s \cosh k_z y$$

The solution for the horizontal coordinate x is:

$$x = -\frac{B_w}{B\rho} \frac{1}{k_z^2} \sin k_z s \cosh k_z y$$

and the normalised momentum is:

$$p_x = -\frac{B_w}{B\rho} \frac{1}{k_z} \cos k_z s \cosh k_z y$$

Vertical focusing in a wiggler

Now we write the vertical equation of motion of a particle in the wiggler:

$$\frac{dp_y}{ds} = \frac{q}{P_0} p_x B_z = \frac{B_w}{B\rho} p_x \cos k_z s \sinh k_z y$$

The total deflection in one period of the wiggler is:

$$\Delta p_y \approx \frac{B_w}{B\rho} \sinh k_z y \int_0^{\lambda_w} p_x \cos k_z s \, ds$$

Using our result for p_x, we have:

$$\Delta p_y \approx -\left(\frac{B_w}{B\rho}\right)^2 \frac{1}{k_z} \sinh k_z y \cosh k_z y \int_0^{\lambda_w} \cos^2 k_z s \, ds = -\frac{\pi}{2k_z^2}\left(\frac{B_w}{B\rho}\right)^2 \sinh 2k_z y$$

Making a series expansion in y we find:

$$\Delta p_y \approx -\frac{\pi}{k_z}\left(\frac{B_w}{B\rho}\right)^2 \left(y + \frac{2}{3} k_z^2 y^3 + \cdots \right)$$

Vertical focusing in a wiggler

Taking the term linear in y, we see that the combination of the "wiggling" trajectory with the longitudinal field component in the wiggler leads to a vertical deflection, equivalent (per period of the wiggler) to a vertically focusing quadrupole with integrated strength:

$$k_1 l = -\frac{\pi}{k_z}\left(\frac{B_w}{B\rho}\right)^2$$

There is also a term cubic in y:

$$\Delta p_y^{(3)} \approx -\frac{2\pi}{3}\left(\frac{B_w}{B\rho}\right)^2 k_z y^3$$

The cubic term is often referred to as the "dynamic octupole" term. Note that the size of this term *increases* as the period of the wiggler *decreases*.

Vertical focusing in a wiggler

Assuming a sinusoidal vertical field in the wiggler, Maxwell's equations impose conditions that require a corresponding sinusoidal longitudinal field. This results in vertical focusing.

An alternative model for a wiggler uses a sequence of "hard edged" dipole magnets, separated by drift spaces. Such a model also produces a vertical focusing: in this case, it comes from the combination of the (thin) fringe fields with the angle between the pole faces and the particle trajectory.

The source of the vertical focusing is fundamentally the same in each model, and we obtain the same vertical focusing strength if we use the same peak field in each case.

Neither model provides any horizontal focusing. However, a real wiggler has a finite pole width. This breaks the horizontal translational symmetry, and can result in horizontal focusing, as we now show…

Horizontal focusing in a wiggler

The finite width of the poles in a wiggler results in a "roll-off" of the field strength with increasing horizontal distance from the axis of the wiggler.

A simple model for the field may be written:

$$B_x = -\frac{k_x}{k_y} B_w \sin k_x x \sinh k_y y \sin k_z z$$

$$B_y = B_w \cos k_x x \cosh k_y y \sin k_z z$$

$$B_z = \frac{k_z}{k_y} B_w \cos k_x x \sinh k_y y \cos k_z z$$

where Maxwell's equations impose the condition:

$$k_x^2 + k_z^2 = k_y^2$$

Horizontal focusing in a wiggler

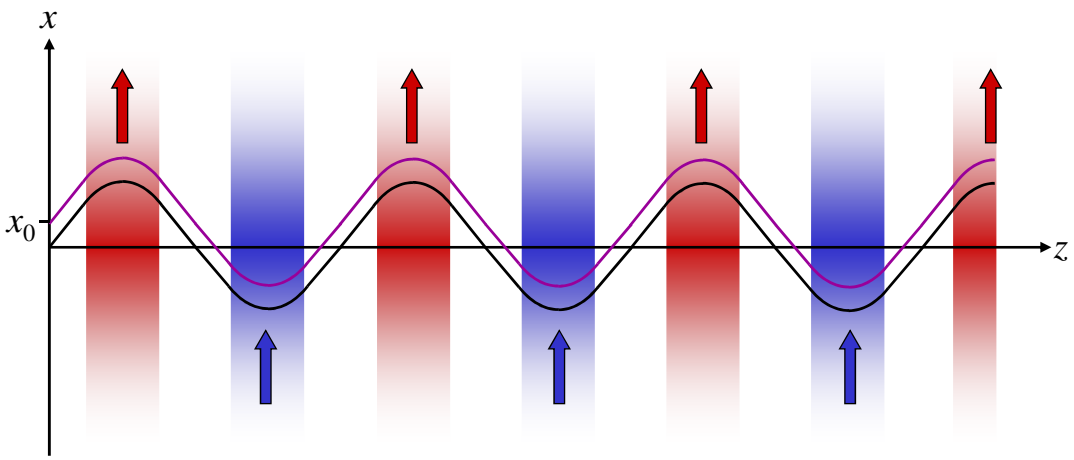

The roll-off in the wiggler field means that a particle with non-zero initial horizontal coordinate sees alternately weaker and stronger fields in successive poles.

The net effect is a horizontal deflection that appears as a horizontal defocusing force.

Horizontal focusing in a wiggler

Consider a particle that follows a trajectory:

$$x = x_0 + \hat{x}\sin k_z s$$

where x_0 is the initial horizontal coordinate, and $\hat{x}$ is the amplitude of the "wiggling" trajectory, given by:

$$\hat{x} = \frac{1}{k_z^2}\frac{B_w}{B\rho}$$

For a particle on the mid-plane $(y = 0)$, we can find the horizontal kick on the particle when it moves through one period of the wiggler from:

$$\begin{aligned}
\Delta p_x &= -\frac{1}{B\rho}\int_0^{\lambda_w} B_y \, ds \\
&= -\frac{B_w}{B\rho}\int_0^{\lambda_w} \cos\left[k_x\left(x_0 + \hat{x}\sin k_z s\right)\right]\sin k_z s \, ds \\
&= \frac{B_w}{B\rho}\lambda_w J_1\left(k_x\hat{x}\right)\sin\left(k_x x_0\right) \\
&\approx \frac{B_w}{B\rho}\lambda_w \frac{k_x\hat{x}}{2}k_x x_0
\end{aligned}$$

Horizontal focusing in a wiggler

Hence we find that the horizontal kick on a particle, resulting from the horizontal roll-off of the wiggler field, is:

$$\Delta p_x \approx \frac{\lambda_w}{2}\left(\frac{B_w}{B\rho}\right)^2 \frac{k_x^2}{k_z^2} x_0$$

The vertical focusing in this case is given by:

$$\Delta p_y \approx -\frac{\lambda_w}{2}\left(\frac{B_w}{B\rho}\right)^2 \frac{k_y}{k_z} y_0$$

For infinitely wide poles, $k_x \to 0$, and there is no horizontal focusing. Also in this case, we have $k_y = k_z$, and the vertical focusing is determined completely by the wiggler period and peak field.

For poles with a finite width, horizontal defocusing is introduced, and there is an enhancement in the vertical focusing, following from:

$$k_y^2 = k_x^2 + k_z^2$$

The horizontal and vertical focusing depend on the wiggler pole width.

Nonlinear effects in wigglers

At the centre of a pole $(\sin k_z s = 1)$ and in the mid-plane $(y = 0)$, the vertical field is given by:

$$B_y = B_w \cos k_x x = B_w\left(1 - \tfrac{1}{2}k_x^2 x^2 + \tfrac{1}{24}k_x^4 x^4 - \cdots\right)$$

The quadratic dependence of the field strength on x leads to the horizontal defocusing: the sextupole component of the field “feeds down” (when combined with the wiggling trajectory) to give a linear focusing effect.

We can expect the decapole component of the field to feed down to give an octupole component, etc. Hence, for finite pole width, a “dynamic octupole” appears in the horizontal plane as well as in the vertical plane.

Wigglers can have a significant impact on the nonlinear dynamics, and (potentially) restrict the dynamic aperture. It is important to have a good model for analysis of the nonlinear effects.

Modelling the nonlinear effects of wigglers

There are four steps in the procedure for modelling the nonlinear effects of wigglers:

1. Use a magnetostatics code (e.g. Radia, Tosca…) to calculate the magnetic field in one periodic section of the wiggler.

2. Fit an analytical model for the field (a mode decomposition) to the field data from the magnetostatics code.

3. From the analytical model, construct a dynamical map describing the motion of a particle through the wiggler (MaryLie, COSY…)

4. Use the dynamical map in a tracking code to determine the impact of the wiggler on the nonlinear dynamics (tune shifts, resonances, dynamic aperture…)

We shall assume step 1 has been done, and look briefly at steps 2-4.

Modelling the nonlinear effects of wigglers: Step 2

We can generalise the representation that we used previously to include a series of wiggler modes:

$$B_x = -B_w \sum_{m,n} c_{m,n} \frac{mk_x}{k_{y,mn}} \sin mk_x x \sinh k_{y,mn} y \sin nk_z z$$

$$B_y = B_w \sum_{m,n} c_{m,n} \cos mk_x x \cosh k_{y,mn} y \sin nk_z z$$

$$B_z = B_w \sum_{m,n} c_{m,n} \frac{nk_z}{k_{y,mn}} \cos mk_x x \sinh k_{y,mn} y \cos nk_z z$$

$$k_{y,mn}^2 = m^2 k_x^2 + n^2 k_z^2$$

If we consider the vertical field on the mid-plane ($y = 0$):

$$B_y = B_w \sum_{m,n} c_{m,n} \cos mk_x x \sin nk_z z$$

we can in principle determine the coefficients c_{mn} by a 2D Fourier transform of the field data. However, in practice, this does not work very well. The hyperbolic dependence of the field on the vertical coordinate means that any small errors from the fit increase exponentially away from the mid-plane.

Modelling the nonlinear effects of wigglers: Step 2

A better technique is to fit the field on a surface enclosing the region of interest. The hyperbolic dependence of the field then means that any small errors in the fit *decrease* exponentially towards the axis of the wiggler.

One possibility is to use a rectangular box: this amounts to fitting the Fourier modes on a planar surface some distance above (or below) the mid-plane. However, the Fourier modes are sinusoidal in the horizontal coordinate x, which does not represent the real field very well.

An alternative technique is to fit the field on a cylindrical surface inscribed in the wiggler aperture. This captures the periodic behaviour of the field in the longitudinal and azimuthal coordinates.

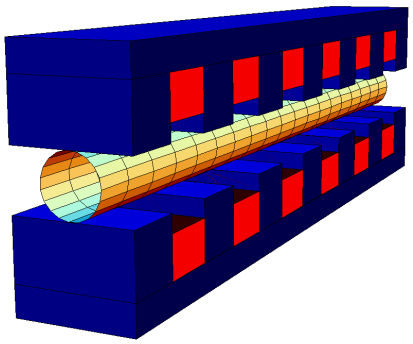

$$B_\rho = \sum_{mn} \alpha_{mn} I'_m(nk_z\rho)\sin m\phi \sin nk_z z$$

$$B_\phi = \sum_{mn} \alpha_{mn} \frac{m}{nk_z\rho} I_m(nk_z\rho)\cos m\phi \sin nk_z z$$

$$B_z = \sum_{mn} \alpha_{mn} I_m(nk_z\rho)\sin m\phi \cos nk_z z$$

Modelling the nonlinear effects of wigglers: Step 2

If we know the radial field component at a fixed radius:

$$B_\rho = \sum_{mn} \alpha_{mn} I'_m(nk_z\rho)\sin m\phi \sin nk_z z$$

we can obtain the mode coefficients α_{mn} by a 2D Fourier transform. This works better than in the Cartesian case, because there is a real periodicity in the azimuthal coordinate.

Usually, we take the surface as close to the pole face as possible (but with caution: sometimes the field data are not reliable very close to the pole face).

The number of modes required to achieve a good fit varies, depending on the shape of the field.

Once we know the mode coefficients α_{mn}, we can construct all the field components at any point. The errors are small within the cylindrical surface used for the fit.

Modelling the nonlinear effects of wigglers: Step 2

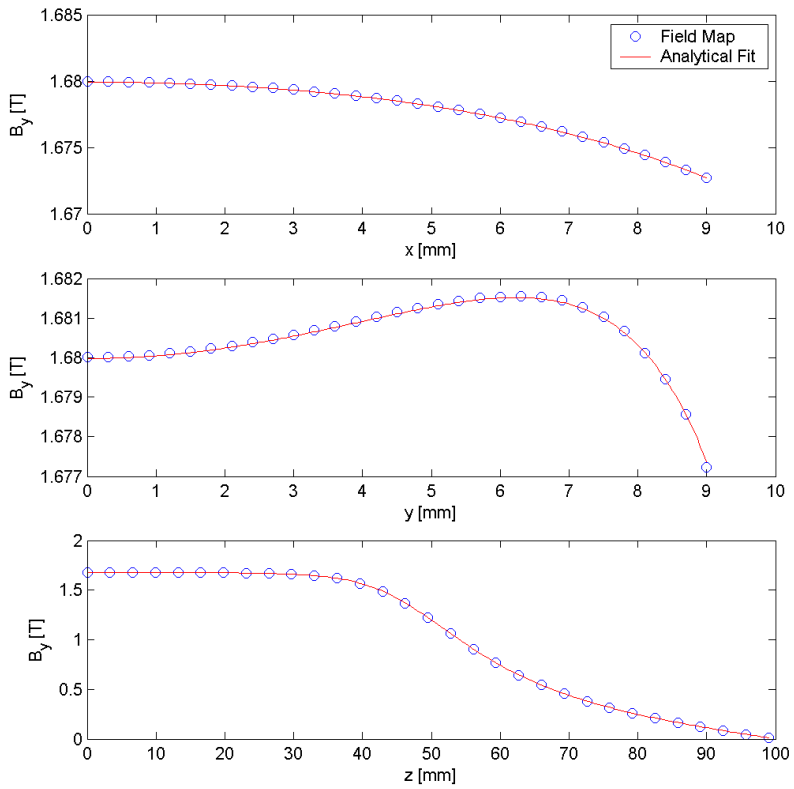

Example:

Fit to a model of a permanent magnet wiggler for the TESLA damping ring.

Mode numbers:

$m_{\max} = 36$

$n_{\max} = 100$

Fit on surface:

$\rho = 9$ mm

Modelling the nonlinear effects of wigglers: Step 2

The residuals of the fit indicate the quality. (Peak field = 1.68 T).

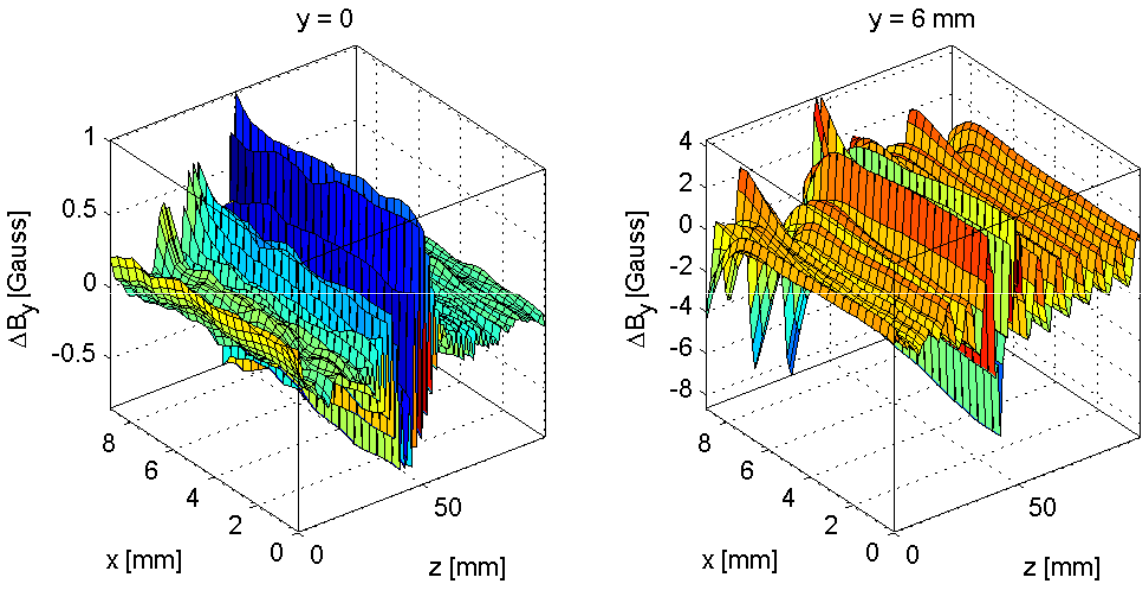

Modelling the nonlinear effects of wigglers: Step 3

Once we have an mode decomposition of the field, we can use an "algebraic" code to construct a dynamical map.

Briefly, an "algebraic" code manipulates algebraic expressions rather than numbers. There are different types of algebraic codes, for example:

- Differential algebra codes (COSY)
  http://bt.pa.msu.edu/index_cosy.htm
- Lie algebra codes (MaryLie)
  http://www.physics.umd.edu/dsat/dsatmarylie.html

A differential algebra (DA) code is capable of manipulating Taylor series. By incorporating an integrator to solve the equations of motion in a magnetic field (given as a mode decomposition) into a DA code, we can construct, for a given field, a Taylor map representing the dynamics of a particle in that field.

Modelling the nonlinear effects of wigglers: Step 3

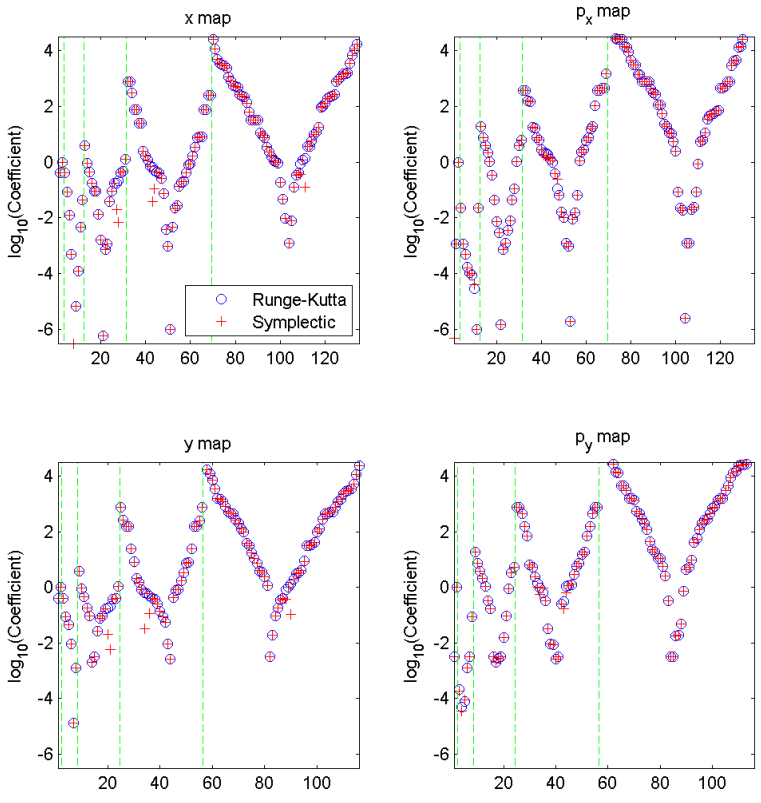

Example of a Taylor map constructed with COSY.

The points represent the coefficients of the different terms in the fifth-order maps for the dynamical variables.

The green lines group terms of the same order.

The results of two different integration algorithms are compared: an explicit symplectic integrator (that requires the paraxial approximation) and a Runge-Kutta integrator.

Modelling the nonlinear effects of wigglers: Step 4

The final step is to take the map constructed using an algebraic code, and include it in a tracking code, to look at the impact on the dynamics.

The simplest analysis is to track particles at different amplitudes, and see which ones survive. This gives a basic measure of the dynamic aperture, but little information on the underlying dynamics.

A more sophisticated technique is that of "frequency map analysis" (FMA). The procedure with FMA is as follows:

- Track a particle through the storage ring for some number of turns, starting from specified coordinates. Record the phase space coordinates after each turn.
- Analyse the turn-by-turn tracking data to determine the tunes with high precision. This may be done, for example, using a Fourier analysis technique including filtering and interpolation.
- Continue tracking for some additional number of turns, then repeat the calculation to find the tunes over the additional turns. Any change in the tunes indicates "diffusion" in tune space.
- Repeat the analysis for a range of initial coordinates, and plot the points in both coordinate space and tune space, using a colour scale to indicate rates of diffusion in tune space.

Wiggler nonlinearities impact the tune-shifts with amplitude

	Linear wiggler model	Nonlinear wiggler model	
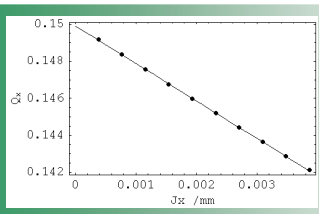	$\frac{\partial Q_x}{\partial J_x} = -2.02\ \mathrm{mm}^{-1}$	$\frac{\partial Q_x}{\partial J_x} = +3.34\ \mathrm{mm}^{-1}$	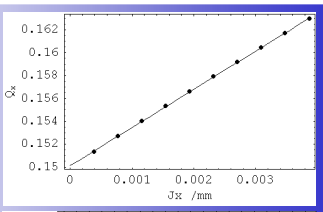
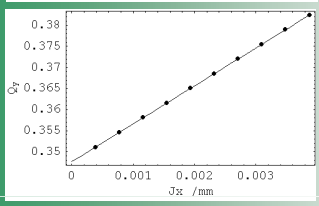	$\frac{\partial Q_y}{\partial J_x} = +8.99\ \mathrm{mm}^{-1}$	$\frac{\partial Q_y}{\partial J_x} = -11.4\ \mathrm{mm}^{-1}$	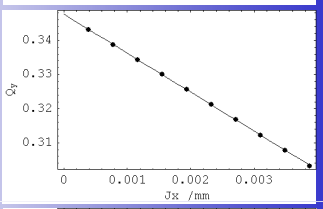
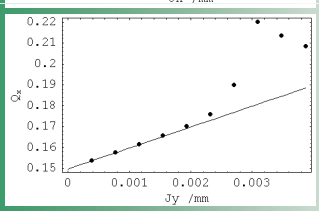	$\frac{\partial Q_x}{\partial J_y} = +9.99\ \mathrm{mm}^{-1}$	$\frac{\partial Q_x}{\partial J_y} = -10.2\ \mathrm{mm}^{-1}$	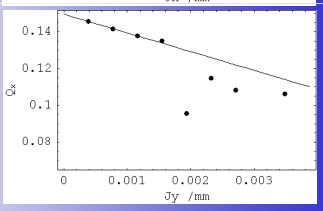
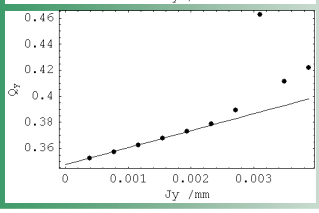	$\frac{\partial Q_y}{\partial J_y} = +13.0\ \mathrm{mm}^{-1}$	$\frac{\partial Q_y}{\partial J_y} = +35.4\ \mathrm{mm}^{-1}$	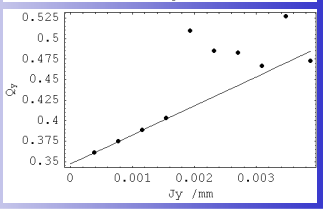

Dynamic aperture of a 6 km ILC damping ring lattice

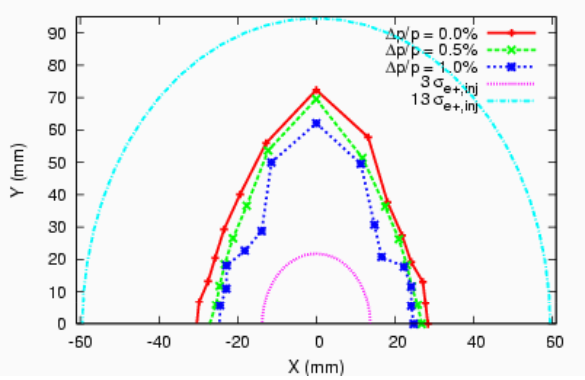

Dynamic aperture with linear wiggler model.

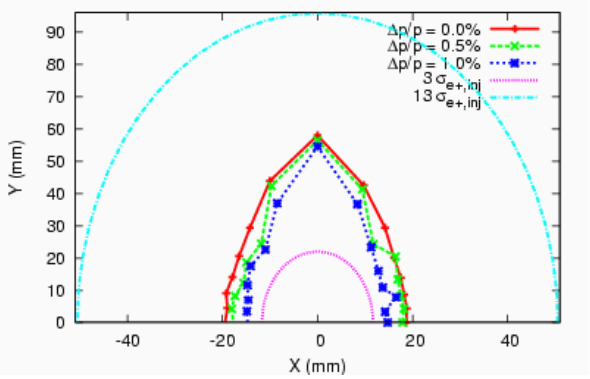

Dynamic aperture with nonlinear wiggler model.

Frequency map analysis of a 6 km ILC damping ring lattice

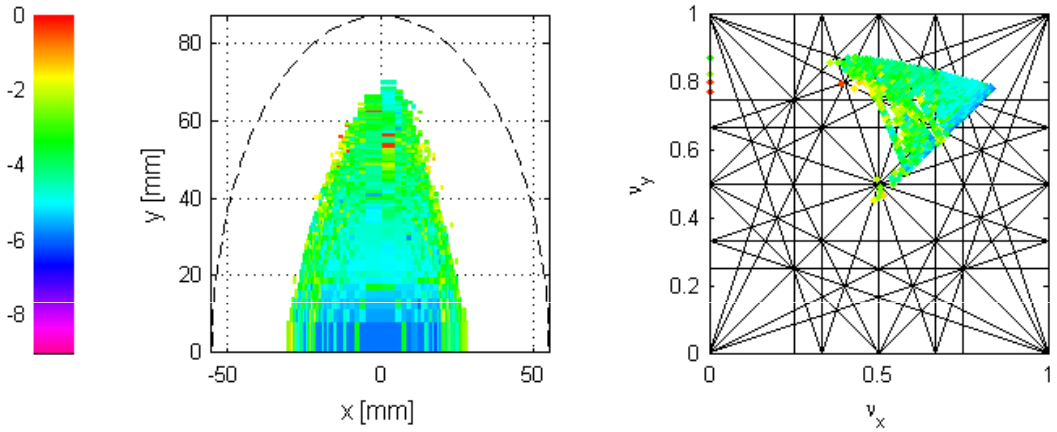

Frequency map of OCS2 lattice including nonlinear wiggler model, computed with COSY/Merlin.

Frequency map analysis of a 6 km ILC damping ring lattice

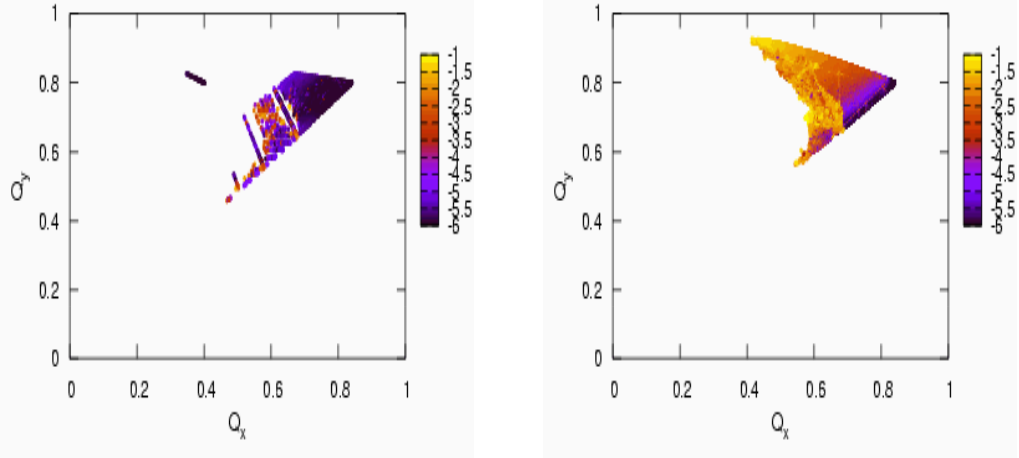

Frequency maps of OCS2 lattice using linear wiggler model (left) and nonlinear wiggler model (right), computed with BMAD.

Acceptance specifications for the damping rings

The dynamic aperture is an important component of the *acceptance* of the ring, which also includes the physical aperture.

The acceptance of the ring is the region of phase space within which particles injected into the ring will stay in the ring long enough to be damped by radiation.

The acceptance specifications for the positron damping ring are particularly demanding, because the injected positron beam will have a very large emittance.

The acceptance for the positron beam is usually specified in terms of the maximum "transverse amplitude", A_x (and A_y) for any particle in the beam:

$$\frac{A_x}{\gamma} = \gamma_x x^2 + 2\alpha_x x p_x + \beta_x p_x^2$$

Longitudinally, the specification is given in terms of the maximum energy deviation of any particle in the beam, i.e. as a *full-width* energy spread.

Injected positron distribution

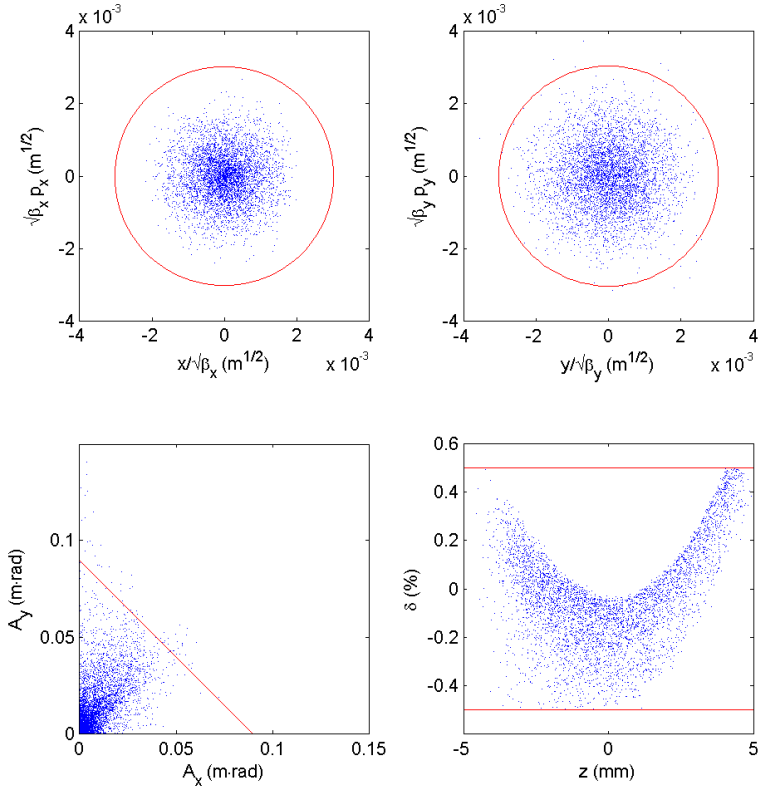

Acceptance specifications

Presently, the acceptance specification for the injected positron beam is:

$$A_x + A_y < 0.09 \text{ m - rad}$$

It is sometimes convenient to work with an "equivalent rms beam size", σ_x. This is defined so that:

$$3\sigma_x = x_{\max}$$

and similarly for y. Since, in the absence of dispersion:

$$\sigma_x = \sqrt{\beta_x \varepsilon_x}$$

where ε_x is the rms emittance:

$$\varepsilon_x = \langle J_x \rangle = \frac{\langle A_x \rangle}{2\gamma}$$

and:

$$x_{\max} = \sqrt{\beta_x \frac{A_{x,\max}}{\gamma}}$$

it follows that:

$$\gamma\varepsilon_x = \frac{1}{9} A_{x,\max}$$

Hence, we sometimes refer to an injected normalised emittance of 0.01 m.

Acceptance specifications

Longitudinally, the injected phase space is likely to be very mismatched, with the injected energy spread much larger in proportion to the injected bunch length, than is the case for the equilibrium beam.

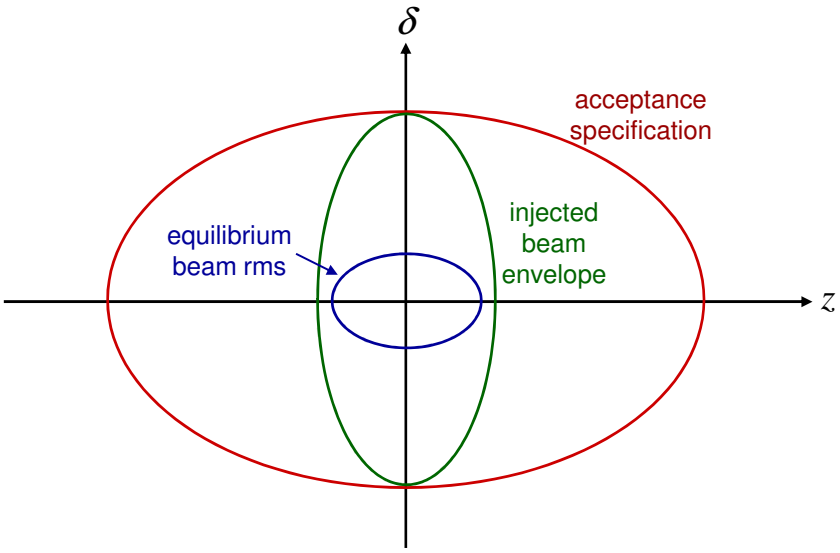

Field errors and dynamic aperture

Generally, the lattice is designed to provide a dynamic aperture significantly larger than the specified acceptance, to allow for magnet field errors that can degrade the dynamic aperture.

Field errors that can affect the dynamic aperture include:

- linear focusing errors (quadrupole strength errors);
- nonlinear fields in the damping wigglers;
- systematic higher-order multipoles in dipoles, quadrupoles, sextupoles (intrinsic to the designs of the magnets);
- random higher-order multipoles in dipoles, quadrupoles, sextupoles (arising from variations in magnet fabrication).

Field errors and dynamic aperture

Multipole field components are conveniently specified in terms of the field strength at a given distance (the "reference radius") from the axis of the magnet:

$$\frac{\Delta B_y + i\Delta B_x}{|B(r_0)|} = \sum_n (b_n + ia_n)\left(\frac{x+iy}{r_0}\right)^{n-1}$$

The coefficients a_n specify the skew multipole components;
the coefficients b_n specify the normal multipole components.

$n = 1$ gives the dipole component;
$n = 2$ gives the quadrupole;
$n = 3$ gives the sextupole, etc.

For systematic errors, the multipole components in all magnets of a given type are determined by fixed values of the coefficients a_n and b_n.

For random errors, the coefficients a_n and b_n give the rms of a distribution of multipole components in a set of magnets of a given type.

Field errors and dynamic aperture

The values of the coefficients a_n and b_n for both systematic and random errors depend on the magnet design.

Important features include:

- the shape of the pole tips;
- the shape of the yoke;
  - higher symmetry helps reduce systematic errors;
- the aperture of the magnet;
  - larger aperture helps reduce multipole components;
- the length of the magnet;
  - fringe fields can be more significant in short magnets.

It is easier to achieve good field quality in a long, large-aperture magnet; unfortunately, these characteristics increase the cost (and, for electromagnets, the power consumption) of the magnet.

Example of field errors in PEP-II magnets

Table 3.2: Sytematic and random multipole errors in the quadrupoles used in tracking studies in the reference lattices. The reference radius is 50 mm.

n	systematic		random	
	b_n	a_n	b_n	a_n
3	-1.24×10^{-5}	-1.15×10^{-5}	7.61×10^{-5}	7.25×10^{-5}
4	2.30×10^{-6}	1.41×10^{-5}	1.32×10^{-4}	1.27×10^{-4}
5	-4.30×10^{-6}	6.20×10^{-7}	1.50×10^{-5}	1.62×10^{-5}
6	3.40×10^{-4}	-4.93×10^{-5}	1.65×10^{-4}	3.63×10^{-4}
7	3.00×10^{-7}	-1.02×10^{-6}	6.70×10^{-6}	6.60×10^{-6}
8	6.00×10^{-7}	3.80×10^{-7}	8.90×10^{-6}	6.60×10^{-6}
9	6.00×10^{-7}	-2.80×10^{-7}	4.60×10^{-6}	4.90×10^{-6}
10	-6.17×10^{-5}	-5.77×10^{-5}	2.46×10^{-4}	2.33×10^{-4}
11	-2.00×10^{-7}	-1.80×10^{-7}	4.20×10^{-6}	3.50×10^{-6}
12	3.60×10^{-6}	-6.53×10^{-6}	3.48×10^{-5}	3.66×10^{-5}
13	6.00×10^{-7}	1.20×10^{-6}	9.20×10^{-6}	8.60×10^{-6}
14	1.00×10^{-6}	-7.40×10^{-7}	4.76×10^{-5}	4.46×10^{-5}

"Allowed" multipoles

Multipole field errors can affect the dynamic aperture

In some cases, multipole field errors can have a significant impact; but if the lattice design is robust, and the field errors are small enough, there should be little overall reduction in the dynamic aperture from higher-order multipoles in the dipoles, quadrupoles and sextupoles.

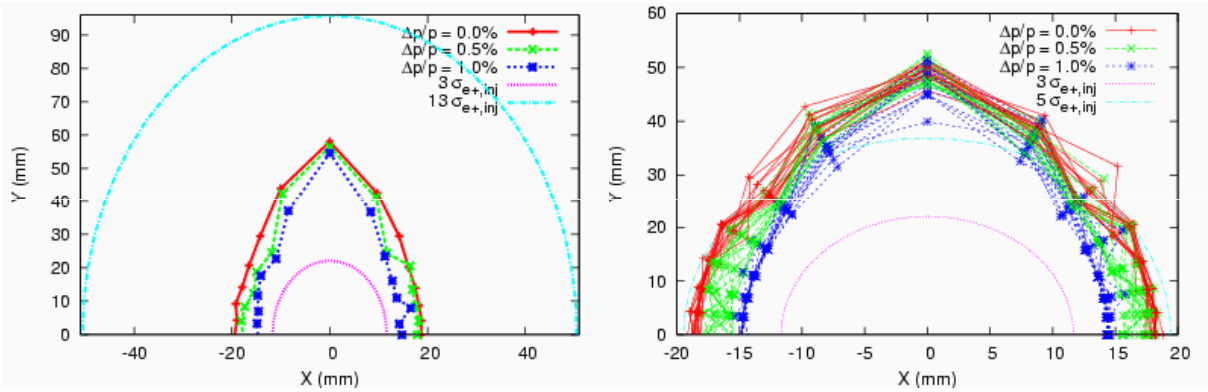

Dynamic aperture in a 6 km ILC damping ring lattice (OCS2) without field errors (left) and with 15 seeds of higher-order multipole errors (right).

Summary

Damping wigglers are used to increase the rate of energy loss from the beam through synchrotron radiation, and hence to reduce the damping times.

In the ILC damping rings, the wigglers dominate the energy loss (producing 90% of the radiation, compared to 10% from the main dipoles), and also affect other dynamical parameters:

- the wigglers have a negligible impact on the momentum compaction factor;
- the wigglers dominate the equilibrium energy spread;
- the wigglers significantly affect the natural emittance, but the arc dipoles also make a significant contribution.

Wiggler fields produce vertical and (for finite pole width) horizontal linear focusing.

The wiggler fields have intrinsically nonlinear components, which must be carefully modelled to determine the impact on the dynamic aperture.

A good dynamic aperture is needed to accept the large injected positron beam. All limitations on the acceptance must be considered, including higher-order multipole field errors in the dipoles, quadrupoles and sextupoles.

Appendix: multipole components in wiggler fields

The strengths of the "dynamic" multipole components in wiggler fields can be estimated from the coefficients of the field decomposition in cylindrical modes.

$$B_\rho = \sum_{mn} \alpha_{mn} I'_m(nk_z\rho)\sin m\phi \sin nk_z z$$

$$B_\phi = \sum_{mn} \alpha_{mn} \frac{m}{nk_z\rho} I_m(nk_z\rho)\sin m\phi \sin nk_z z$$

$$B_z = \sum_{mn} \alpha_{mn} I_m(nk_z\rho)\sin m\phi \cos nk_z z$$

By considering the variation of the radial component of the field, B_ρ with the azimuthal angle ϕ, we see that:

$m = 1$ gives the dipole component of the field;

$m = 2$ gives the quadrupole component of the field;

$m = 3$ gives the sextupole component of the field…

In a wiggler with symmetry under $x \rightarrow -x$, only components with odd values of m are allowed.

Appendix: multipole components in wiggler fields

The horizontal deflection of a particle moving through one wiggler period in the horizontal mid-plane is:

$$\Delta p_x = \frac{1}{B\rho}\int_0^{\lambda_w} B_\phi \, ds$$

Expanding the Bessel function to lowest order in ρ, the azimuthal component of the field from the mode with a given m and with $n=1$ is:

$$B_\phi \approx \alpha_{m1}\frac{m}{2^m\Gamma(m+1)}(k_z\rho)^{m-1}\sin\left(m\frac{\pi}{2}\right)\cos k_z z$$

Appendix: multipole components in wiggler fields

For a particle moving in the horizontal mid-plane of the wiggler, we can write:

$$\rho = x_0 + a\sin k_z s$$

Substituting this into the expression for the azimuthal component of the magnetic field, we find that the vertical field seen by the particle along its trajectory is:

$$B_\phi \approx \alpha_{m1}\frac{m(k_z a)^{m-1}}{2^m\Gamma(m+1)}\left[\frac{x}{a}+\cos(k_z z)\right]^{m-1}\sin\left(m\frac{\pi}{2}\right)\cos k_z z$$

$$\approx \alpha_{m1}\frac{m(k_z a)^{m-1}}{2^m\Gamma(m+1)}\left[\left(\frac{x}{a}\right)^{m-1}\cos k_z z+(m-1)\left(\frac{x}{a}\right)^{m-2}\cos^2 k_z z+\ldots\right]\sin\left(m\frac{\pi}{2}\right)$$

Performing the integral, we find that the deflection of the particle is:

$$\Delta p_x = \frac{1}{B\rho}\int_0^{\lambda_w} B_\phi \, ds \approx \frac{1}{B\rho}\alpha_{m1}\frac{m(m-1)(k_z a)^{m-1}}{2^{m+1}\Gamma(m+1)}\left[\left(\frac{x}{a}\right)^{m-2}+\ldots\right]\sin\left(m\frac{\pi}{2}\right)$$

Hence, we find that:

the $m = 3$ (sextupole) component gives a deflection $\propto x$ (dynamic quadrupole);

the $m = 5$ (decapole) component gives a deflection $\propto x^3$ (dynamic octupole)…